Astrophysical Journal, to appear in January 10, 2000 issue, Vol. 528
Preprint typeset using LaTeX style apjgalley

INVERSE BREMSSTRAHLUNG IN SHOCKED ASTROPHYSICAL PLASMAS

Matthew G. Baring[1] and Frank C. Jones
Laboratory for High Energy Astrophysics, Code 661,
NASA Goddard Space Flight Center, Greenbelt, MD 20771, U.S.A.
baring@lheavx.gsfc.nasa.gov, frank.c.jones@gsfc.nasa.gov
AND
Donald C. Ellison
Department of Physics, North Carolina State University,
Box 8202, Raleigh NC 27695, U.S.A.
don_ellison@ncsu.edu
Astrophysical Journal, to appear in January 10, 2000 issue, Vol. 528

ABSTRACT

There has recently been interest in the role of inverse bremsstrahlung, the emission of photons by fast suprathermal ions in collisions with ambient electrons possessing relatively low velocities, in tenuous plasmas in various astrophysical contexts. This follows a long hiatus in the application of suprathermal ion bremsstrahlung to astrophysical models since the early 1970s. The potential importance of inverse bremsstrahlung relative to normal bremsstrahlung, i.e. where ions are at rest, hinges upon the underlying velocity distributions of the interacting species. In this paper, we identify the conditions under which the inverse bremsstrahlung emissivity is significant relative to that for normal bremsstrahlung in shocked astrophysical plasmas. We determine that, since both observational and theoretical evidence favors electron temperatures almost comparable to, and certainly not very deficient relative to proton temperatures in shocked plasmas, these environments generally render inverse bremsstrahlung at best a minor contributor to the overall emission. Hence inverse bremsstrahlung can be safely neglected in most models invoking shock acceleration in discrete sources such as supernova remnants. However, on scales $\gtrsim 100\,$pc distant from these sources, Coulomb collisional losses can deplete the cosmic ray electrons, rendering inverse bremsstrahlung, and perhaps bremsstrahlung from knock-on electrons, possibly detectable.

Subject headings: acceleration of particles — cosmic rays — supernova remnants — radiation mechanisms: non-thermal — gamma-rays: theory

1. INTRODUCTION

The process of inverse bremsstrahlung has received attention from time to time over the last three decades, in various astrophysical settings. Inverse bremsstrahlung is defined here to be the emission of a single photon when a high speed ion collides with an electron that is effectively at rest, and has often been referred to as suprathermal proton bremsstrahlung (e.g. Boldt & Serlemitsos 1969; Brown 1970; Jones 1971; Haug 1972). Being a kinematic inverse (an analogy can be drawn with inverse Compton scattering) arising purely via Lorentz transformations between reference frames (i.e. it is still the electron that radiates), it is not to be confused with the true quantum electrodynamical inverse of conventional bremsstrahlung, namely the absorption of photons in 3-body collisions with electrons and ions, a process that is highly improbable in tenuous (i.e. optically thin) astrophysical plasmas.

The first application of suprathermal proton bremsstrahlung in astrophysical models dates to the work of Hayakawa & Matsuoka (1964), which considered such radiation in collisions between cosmic rays and ambient electrons in the intergalactic medium as a source of the cosmic X-ray background (XRB) at energies $\lesssim 10\,$keV. This concept was developed in the papers by Hayakawa (1969), Boldt & Serlemitsos (1969), and Brown (1970), with Boldt & Serlemitsos proposing that suprathermal proton bremsstrahlung could account for the flat spectral index of the XRB below around 15 keV, while noting that an unusually high column density of ambient electrons would be required to match the observed flux. The interest in the relevance of inverse bremsstrahlung to the cosmic XRB has since diminished, and more recent opinion favours the accumulation of unresolved discrete sources as the dominant contributions (see Fabian & Barcons 1992, for a comprehensive review). Although thermal bremsstrahlung at around 40 keV can fit the 2–100 keV spectrum fairly well (Marshall, et al. 1980; see also Boldt 1987, for a review), recent critical evidence limits the contribution of truly diffuse emission from the intergalactic medium to less than 0.01% of the observed flux. This bound is derived from upper limits to the mean cosmological electron density obtained from the measurements of COBE to Compton scattering-induced distortion of the cosmic microwave background (Wright, et al. 1994).

Renewed interest in inverse bremsstrahlung has arisen in the last year. Tatischeff, Ramaty & Kozlovsky (1998) and Dogiel et al. (1998) have discussed expectations for suprathermal proton bremsstrahlung in the X-ray band, assuming a significant enhancement of the density of low energy cosmic ray ions in the Orion region. Inferences of such an abundance of ions were drawn from the reported (e.g. Bloemen et al. 1994), but recently retracted (Bloemen et al. 1999), detection with COMPTEL/CGRO of emission lines from the Orion molecular cloud complex; these were attributed to Carbon and Oxygen nuclear line emission in collisions with ambient ions. In a different context, Valinia and Marshall (1998) conjectured that inverse bremsstrahlung from cosmic rays could be responsible for much of the diffuse X-ray emission seen in the galactic ridge. Pohl (1998) has responded to this proposition by

[1]Universities Space Research Association

arguing that it is difficult to produce the diffuse component in the ridge via inverse bremsstrahlung without violating observational limits to nuclear excitation line and pion decay continuum emission. Furthermore, Tatischeff, Ramaty & Valinia (1999) argue that by normalizing the low energy cosmic ray ion populations using the galactic Be production rate, the contribution of inverse bremsstrahlung to the thin disk component of unresolved/diffuse 10-60 keV emission detected by RXTE is at most a few percent.

The focus of the presentation here is on collisionless shocked astrophysical plasmas, which distinguish themselves from the diffuse emission scenarios addressed by Valinia and Marshall (1998), Pohl (1998) and Tatischeff, Ramaty & Valinia (1999) by the insignificance of Coulomb collisions compared to interactions between the magnetic field and charged particles. The principal examples in mind here are young supernova remnants, i.e. those perhaps mature enough to be in the Sedov epoch, but well before the radiative phase. The bremsstrahlung emission properties of shocked environments are dictated by the dissipation between ions and electrons in the shock layer. We show in Section 2 that only when electron and ion thermal speeds are comparable (i.e., when the temperature ratio is on the order of, or less than the mass ratio, $T_e/T_p \lesssim m_e/m_p$) can inverse bremsstrahlung contribute significantly relative to normal electron bremsstrahlung in the optical, X-ray and gamma-ray wavebands. We argue in Subsection 2.4 that such conditions are not easily realized in the majority of *shocked* astrophysical environments, thereby rendering suprathermal proton bremsstrahlung unimportant for most discrete sources. By extension, the importance of inverse bremsstrahlung as a continuum emission mechanism in extended regions is contingent upon there being a relative paucity of primary cosmic ray electrons in the interstellar medium on appropriate length scales ($\gtrsim 100\,\mathrm{pc}$). This point, and the role of knock-on electron bremsstrahlung, are discussed in Section 3.

2. INVERSE BREMSSTRAHLUNG VERSUS ELECTRON BREMSSTRAHLUNG

The key question of interest to astrophysicists that we address here is when the inverse bremsstrahlung process is significant relative to the normal bremsstrahlung mechanism in shocked astrophysical plasmas. Clearly, the relative numbers of projectile and target particles will be central to answering this question. Here we aim to determine how such numbers and the associated emissivities for the two processes depend on standard plasma parameters. The emissivities, or photon production rates for either process, can be written in the form

$$\frac{dn_\gamma(\omega)}{dt} \;=\; n_t \int_0^\infty dp\, n_{\rm CR}(p)\, c\beta\, \frac{d\sigma}{d\omega} \quad , \tag{1}$$

for shock-accelerated cosmic ray (projectile) particles with momentum distribution $n_{\rm CR}(p)$ colliding with targets of density n_t that are effectively at rest in the observer's frame. Here $d\sigma/d\omega$ is the cross-section, differential in the photon energy, where we adopt the convention of using dimensionless units throughout this paper: photon energies E_γ are expressed in units of the electron rest mass $m_e c^2$, i.e., via $\omega = E_\gamma/(m_e c^2)$. Hence $d\sigma/d\omega$ has c.g.s. units of cm^2. Also, $c\beta$ is the speed of the projectile of momentum p.

The distribution functions of accelerated particles in shock environs need to be described numerically, in general, as will be evident from the Monte Carlo-generated distributions illustrated later in the paper. However, we can provide a good estimate of the relative importance of inverse bremsstrahlung and classical bremsstrahlung using simple but representative analytic forms for the particle distribution functions. For these purposes, let us approximate the cosmic ray (shock-accelerated) proton and electron distributions in a discrete source by power-laws in momentum, broken at thermal energies. Defining $c\beta_{{\rm T},p}$ and $c\beta_{{\rm T},e}$ to be the proton and electron thermal speeds, respectively, their momentum distributions can be cast in the approximate form

$$n_s(p) \;=\; \frac{n_s}{p_{{\rm T},s}}\;\frac{3(\Gamma_s-1)}{\Gamma_s-1+3\epsilon_s}\begin{cases}\left(\dfrac{p}{p_{{\rm T},s}}\right)^2, & p \le p_{{\rm T},s}\\[2ex] \epsilon_s\left(\dfrac{p}{p_{{\rm T},s}}\right)^{-\Gamma_s}, & p > p_{{\rm T},s}\end{cases} \tag{2}$$

where $p_{{\rm T},s} = m_s c\beta_{{\rm T},s}$ is the thermal (non-relativistic) momentum for species s $(= e, p)$. Here, n_s represents the total density and Γ_s is the power-law index of a given *projectile* species. This discontinuous "schematic" form is chosen to mimic the *slopes* of the low momentum portion of a Maxwell-Boltzmann distribution and the non-thermal suprathermal portion of the cosmic ray distribution, and hence does not accurately describe the spectral structure near the thermal peak. Consideration of such spectral details, which depend on the nature of dissipation in the shock layer, would introduce only modest corrections to the rates derived below, and are immaterial to the qualitative conclusions of this paper. The factor ϵ_s is introduced to account for the fact that the non-thermal tail does not extrapolate directly from the thermal peak in shock acceleration-generated populations, and its values $\lesssim 1$ define the efficiency of the acceleration mechanism, which can be a strong function of the field obliquity (e.g. Baring, Ellison & Jones 1993) and the strength of particle scattering (e.g. Ellison, Baring & Jones 1996) in the shock environs. For ions, acceleration is generally quite efficient, implying $\epsilon_p \sim 0.1$. For electrons, the situation is less clear, pertaining to the well-known electron injection problem in non-relativistic shocks. However, as will be mentioned in Subsection 2.4 below, the observed electron-to-proton cosmic ray abundance ratio provides a canonical lower bound to the injection efficiency of electrons, and generally implies that ϵ_e cannot be dramatically less than ϵ_p. Finally, note that the target density of cool particles for the two processes in question will be written as n_t, and will represent a subset of either of the accelerated populations that are formed from the shock heating of the interstellar medium.

2.1. *The Bremsstrahlung Ratio in a Nutshell*

The ratio $\mathcal{R}_{\rm O-X}$ of inverse bremsstrahlung to bremsstrahlung emission in the optical to X-ray and soft gamma-ray bands can be quickly written down without the encumbrance of the mathematical complexity of the differential cross-sections involved. Here

we enunciate this, the principal result of the paper in a simple and enlightening manner, so that the detailed expositions of the next two subsections can be bypassed by the reader, if desired. At energies below around a few hundred keV, the waveband of interest to the discussions of Boldt & Serlemitsos (1969), Hayakawa (1969), Brown (1970), Tatischeff, Ramaty & Kozlovsky (1998), Dogiel et al. (1998) and Valinia and Marshall (1998), the non-relativistic differential cross-section in Eq. (4) below is operable, and applies to both bremsstrahlung and inverse bremsstrahlung. This cross-section is a function only of the speed of the ballistic particle involved, for a given photon energy. Hence, any disparity in the emissivities for the two processes can only be due to differences in the numbers of ballistic protons and electrons at a given speed, a property that does not extend to relativistic domains. Since bremsstrahlung X-rays in supernova remnant shocks are generally produced by slightly superthermal electrons, this number is just $n_e\epsilon_e/\beta_{\rm T,}{}_e$, reflecting the efficiency of injection into the shock acceleration process. For protons, whose thermal speeds are much lower, only a small fraction can participate in inverse bremsstrahlung collisions with shocked electrons, namely those with speeds exceeding the electron thermal speed $\beta_{\rm T,}{}_e$. Using the suprathermal portion of Eq. (2), this constitutes a "density" $n_p\epsilon_p\,\beta_{{\rm T,}p}^{\Gamma_p-1}\beta_{{\rm T,}e}^{-\Gamma_p}$, so that it immediately follows that the ratio of the two processes is of the order of

$$\mathcal{R}_{\rm O-X} \;=\; \frac{\epsilon_p}{\epsilon_e}\,\left(\frac{\beta_{{\rm T,}p}}{\beta_{\rm T,}{}_e}\right)^{\Gamma_p-1} \quad , \tag{3}$$

for $n_e \sim n_p$, as required by charge neutrality. Therein lies the principal result, borne out in the derivations of the next two subsections, which are expounded because of their usefulness in astrophysical problems. Clearly, the ratio $\mathcal{R}_{\rm O-X}$ depends principally on the degree of temperature equilibration, or otherwise, in the shocked plasma.

2.2. *Radiation from Non-relativistic Particles*

A more-detailed estimate of the relative importance of inverse bremsstrahlung and classical bremsstrahlung at optical to X-ray energies can be obtained by considering only non-relativistic accelerated ions, i.e. those with $\beta \ll 1$. In this regime, the differential cross-section $d\sigma/d\omega$ for either bremsstrahlung or its inverse can be obtained from textbooks such as Jauch and Rohrlich (1980), and is the non-relativistic specialization of the Bethe-Heitler formula:

$$\left.\frac{d\sigma}{d\omega}\right|_{\rm BH} \;=\; \frac{16}{3}\,Z^2\,\frac{\alpha_{\rm f}\,r_0^2}{\omega}\,\frac{1}{\beta^2}\,\log_e\frac{\beta+\sqrt{\beta^2-2\omega}}{\beta-\sqrt{\beta^2-2\omega}} \quad , \quad 2\pi\alpha_{\rm f}Z \lesssim \beta \ll 1 \ , \tag{4}$$

where $\alpha_{\rm f} = e^2/(\hbar c)$ is the fine structure constant, $+Ze$ is the nuclear charge, and $r_0 = e^2/(m_e c^2)$ is the classical electron radius. Here β is the relative speed (in units of c) between the projectile and target, namely the electron speed for classical bremsstrahlung, and the proton (or ion) speed for the inverse process. The applicability of this formula, which is integrated over final electron and photon angles, for both bremsstrahlung and its inverse follows from the Lorentz invariance of the total cross-section σ and the effective invariance of photon angles and energies in non-relativistic transformations between the proton and electron rest frames. With this interpretation, $c\sqrt{\beta^2-2\omega}$ represents the final electron speed in the proton rest frame for either process. Note that Eq. (4) is derived in the Born or plane-wave approximation, and is strictly not applicable to regimes where $\beta \lesssim 2\pi\alpha_{\rm f}Z$ or $\omega \ll \beta^2 \ll 1$ where Coulomb perturbations to the electron wave-functions become important (see the end of this section). Appropriate results for low frequencies and classical regimes can be found in Gould (1970), and references therein, and amount to modifications of the argument of the logarithm.

Using Equation (1), it is straightforward to write down production rates of photons for the two processes in the limit of non-relativistic projectile speeds. For regular bremsstrahlung, the vast majority of shock-accelerated protons are effectively cold due to their generally low thermal speed (except for unusually hot proton components in tenuous plasmas), so that the proton density n_p represents the target density n_t . Hence the photon production rate is

$$\left.\frac{dn_\gamma(\omega)}{dt}\right|_{\rm brems} \;\approx\; \frac{16}{3}\,\frac{n_p n_e}{\beta_{\rm T,}{}_e}\,Z^2\,\frac{\alpha_{\rm f}\,r_0^2 c}{\omega}\,\frac{3(\Gamma_e-1)}{\Gamma_e-1+3\epsilon_e}\,\Big\{f_1(\omega,\,\beta_{\rm T,}{}_e,\,\Gamma_e)+\epsilon_e\,f_2(\omega,\,\beta_{\rm T,}{}_e,\,\Gamma_e)\Big\} \quad , \tag{5}$$

where Γ_e is the electron power-law spectral index, and

$$\begin{aligned} f_1(\omega,\,\beta_{\rm T},\,\Gamma) \;&=\; \frac{1}{\beta_{\rm T}^2}\int_{\sqrt{2\omega}}^{\beta_c} d\beta\,\beta\,\log_e\frac{\beta+\sqrt{\beta^2-2\omega}}{\beta-\sqrt{\beta^2-2\omega}} \\ &=\; \frac{1}{\beta_{\rm T}^2}\left\{(\beta_c^2-\omega)\log_e\frac{\beta_c+\sqrt{\beta_c^2-2\omega}}{\sqrt{2\omega}}-\frac{\beta_c}{2}\,\sqrt{\beta_c^2-2\omega}\right\} \ , \\ f_2(\omega,\,\beta_{\rm T},\,\Gamma) \;&=\; \beta_{\rm T}^{\Gamma}\int_{\beta_c}^{1}\frac{d\beta}{\beta^{1+\Gamma}}\,\log_e\frac{\beta+\sqrt{\beta^2-2\omega}}{\beta-\sqrt{\beta^2-2\omega}} \ , \end{aligned} \tag{6}$$

for

$$\beta_c \;=\; \max\Big\{\,\beta_{\rm T},\;\sqrt{2\omega}\,\Big\}\,. \tag{7}$$

Here we use the argument Γ to represent either Γ_e or Γ_p , as the case may be, in the work below. The first integral in Equation (6) specializes to $[\log_e(2\beta_{\rm T}^2/\omega)-1]/2$ in the limit of $\beta_{\rm T}^2 \gg \omega$. The second integral in Equation (6) is generally expressible in terms

of hypergeometric functions, though such a manipulation is not enlightening. Specialization to the $\beta_{\rm T}^2 \gg \omega$ limit yields tractable integrals and the result $[\log_e(2\beta_{\rm T}^2/\omega) + 2/\Gamma]/\Gamma$. However, remembering that modest corrections to the cross-section in Equation (4) are required (Gould 1970) in this low frequency limit, we restrict use of this specialization to the range $\beta_{\rm T}^2 \gtrsim \omega$. The other interesting limit is when $\beta_{\rm T}^2 \ll \omega \ll 1$, for which only the second integral contributes; the result in this case is $f_2(\omega,\, \beta_{\rm T},\, \Gamma) \approx 2^{\Gamma-2}\, B(\Gamma,\, \Gamma)$, where $B(x, x)$ is the beta function. The substitutions $\beta = \sqrt{2\omega}\,\cosh\theta$, and identity 3.512.1 in Gradshteyn and Ryzhik (1980) facilitate these developments. The limiting cases can then be summarized as

$$\left.\frac{dn_\gamma(\omega)}{dt}\right|_{\rm brems} \approx 16\,\frac{\Lambda}{\beta_{{\rm T},e}}\,\frac{\Gamma_e - 1}{\Gamma_e - 1 + 3\epsilon_e}\,\begin{cases} \dfrac{1}{\omega}\left\{\left(\dfrac{1}{2} + \dfrac{\epsilon_e}{\Gamma_e}\right)\log_e\dfrac{2\beta_{{\rm T},e}^2}{\omega} - \dfrac{1}{2} + \dfrac{2\epsilon_e}{\Gamma_e^2}\right\}, & \omega \lesssim \beta_{{\rm T},e}^2 \ll 1, \\ \epsilon_e\,\dfrac{2^{\Gamma_e/2-1}}{\omega^{1+\Gamma_e/2}}\,\beta_{{\rm T},e}^{\Gamma_e}\,\dfrac{\Gamma^2(\Gamma_e)}{\Gamma(2\Gamma_e)}\ , & \beta_{{\rm T},e}^2 \ll \omega \ll 1, \end{cases} \tag{8}$$

where $\Gamma(x)$ is the Gamma function, and

$$\Lambda \;=\; Z^2 n_p n_e \alpha_{\rm f}\, r_0^2 c \tag{9}$$

defines the fundamental scale for the bremsstrahlung emissivity (i.e. at $\omega \sim 1$ and $\beta_{\rm T} \sim 1$). The ω^{-1} behaviour at low energies reflects the convolution of the bremsstrahlung infra-red divergence with a distribution possessing a finite number of particles. The $\omega^{-(1+\Gamma_e/2)}$ dependence above electron thermal energies arises because the bremsstrahlung flux spectrum traces the electron *energy* distribution. Note that Eq. (8) is strictly valid only when $\Gamma_e > 1$, which will always be the case for convergent electron distributions. A simplified derivation of the form of Eq. (8) is presented in the Appendix.

The inverse bremsstrahlung spectrum can be evaluated in a similar manner, but noting that zero contribution arises whenever the proton speed drops below the electron thermal speed; such a domain of phase space corresponds to normal bremsstrahlung. Hence, thermal protons are never sampled unless the proton thermal speed is comparable to that of the electrons. It follows that the emissivity resembles the form in Equation (5) with just an f_2-type term; extracting the appropriate power-law factor, the inverse bremsstrahlung emissivity can be written

$$\left.\frac{dn_\gamma(\omega)}{dt}\right|_{\substack{\rm inv\\ \rm brems}} \approx \frac{16}{3}\,\frac{n_p n_e}{\beta_{{\rm T},p}}\,Z^2\,\frac{\alpha_{\rm f}\, r_0^2 c}{\omega}\,\frac{3(\Gamma_p - 1)}{\Gamma_p - 1 + 3\epsilon_p}\left(\frac{\beta_{{\rm T},p}}{\beta_{{\rm T},e}}\right)^{\Gamma_p}\epsilon_p\, f_2(\omega,\, \beta_{{\rm T},e},\, \Gamma_p) \quad , \tag{10}$$

where Γ_p is the proton power-law index. The limiting forms of the f_2 function are just as for the bremsstrahlung case, so that we quickly arrive at the limits

$$\left.\frac{dn_\gamma(\omega)}{dt}\right|_{\substack{\rm inv\\ \rm brems}} \approx 16\,\frac{\Lambda}{\beta_{{\rm T},e}}\,\frac{\Gamma_p - 1}{\Gamma_p - 1 + 3\epsilon_p}\left(\frac{\beta_{{\rm T},p}}{\beta_{{\rm T},e}}\right)^{\Gamma_p - 1}\,\begin{cases} \dfrac{1}{\omega}\,\dfrac{\epsilon_p}{\Gamma_p}\left\{\log_e\dfrac{2\beta_{{\rm T},e}^2}{\omega} + \dfrac{2}{\Gamma_p}\right\}, & \omega \lesssim \beta_{{\rm T},e}^2 \ll 1, \\ \epsilon_p\,\dfrac{2^{\Gamma_p/2-1}}{\omega^{1+\Gamma_p/2}}\,\beta_{{\rm T},e}^{\Gamma_p}\,\dfrac{\Gamma^2(\Gamma_p)}{\Gamma(2\Gamma_p)}\ , & \beta_{{\rm T},e}^2 \ll \omega \ll 1. \end{cases} \tag{11}$$

The two photon ranges of interest here, namely $\omega \lesssim \beta_{{\rm T},e}^2 \ll 1$ and $\beta_{{\rm T},e}^2 \ll \omega \ll 1$, are the same as those for bremsstrahlung. This is due in part to the fact that only protons with speeds above electron thermal speeds will participate in inverse bremsstrahlung interactions. Note that relaxing the $\beta_p \gtrsim \beta_{{\rm T},e}$ requirement to bounds on β_p greater than $\beta_{{\rm T},e}$ would introduce the appropriate numerical factor in Equation (11). Clearly, the factor $[\epsilon_p/\epsilon_e](\beta_{{\rm T},p}/\beta_{{\rm T},e})^{\Gamma_p - 1}$ roughly defines the ratio of inverse bremsstrahlung to bremsstrahlung emissivities; expectations for its value in shocked plasmas will form the center of the discussion in Section 2.4 below.

It is salient to remark at this point that the differential cross-section in Equation (4) that we are using (and also the ultra-relativistic limit in Eq. (14) below of the Bethe-Heitler result) was obtained from QED calculations in the Born approximation. At non-relativistic speeds, the Coulomb potential of the target electron or ion perturbs the projectile electron wave-function sufficiently that the plane-wave approximation breaks down. This occurs when $p_e\, x$ drops below $\hbar$, where $p_e = \beta m_e c$ is the momentum of the energetic electron. Here x is the spatial scale appropriate to the interaction, which is the classical electron radius r_0. Hence, so-called Coulomb corrections become necessary when $\beta \lesssim \alpha_{\rm f} = e^2/(\hbar c)$. In such cases, the matrix element for scattering must be determined using Coulomb wave functions. This has been done exactly for non-relativistic electrons colliding with nuclei by Sommerfeld (1931), leading to the application of a simple corrective multiplicative factor (Elwert 1939)

$$\mathcal{C}_{\rm SE}(\beta,\, \omega) \;=\; \frac{\beta}{\beta'}\,\frac{1 - \exp\left[-2\pi\alpha_{\rm f} Z/\beta\right]}{1 - \exp\left[-2\pi\alpha_{\rm f} Z/\beta'\right]} \quad , \quad \beta' = \sqrt{\beta^2 - 2\omega}\ , \tag{12}$$

known as the Sommerfeld-Elwert factor, to the Bethe-Heitler cross-section:

$$\left.\frac{d\sigma}{d\omega}\right|_{\rm SE} \;=\; \mathcal{C}_{\rm SE}(\beta,\, \omega)\,\left.\frac{d\sigma}{d\omega}\right|_{\rm BH} \tag{13}$$

Here β' is the electron's speed (in units of c) in the nuclear rest frame after collision, and Z is the charge number of the nucleus. Note that a similar factor can be employed for electron-electron collisions (Maxon and Corman 1967, see also Haug 1975).

Such factors become important for projectile electron speeds below around $c/10$ (for proton targets). When $\beta_{\mathrm{T},e} \ll 2\pi\alpha_{\mathrm{f}}Z$, the Coulomb correction factor is simply $\beta/\sqrt{\beta^2 - 2\omega}$, and it propagates through all the integrands of the above developments. It is then quickly ascertained that in the $\omega \lesssim \beta_{\mathrm{T},e}^2 \ll 1$ limiting cases, the correction factor is close to unity and therefore can be neglected (modest low frequency corrections for $\omega \ll \beta^2$ are discussed in Gould 1970). For higher photon energies, the Coulomb corrections should be included, with the appropriate modification to the algebraic manipulations. While the resulting integral is not tractable except in terms of higher order hypergeometric functions, we determined numerically that the corrective factor that should be applied to the $\beta_{\mathrm{T},e}^2 \ll \omega \ll 1$ cases in Equations (8) and (11) increases monotonically from 1.17 to 1.94 as Γ_e or Γ_p vary between 1 to 5, the representative range of power-law distribution indices. Since such factors are of the order of unity, we can assert that Coulomb correction factors are only marginally important for bremsstrahlung computations, and will prove immaterial to the considerations and conclusions of this paper; we neglect them in the algebraic expressions hereafter.

2.3. *Emission from Ultra-relativistic Species*

Hard X-rays and gamma-rays from bremsstrahlung and inverse bremsstrahlung are generated by ultra-relativistic electrons and ions. In this regime, a single cross-section cannot be used for the two mechanisms due to the introduction of aberrations in photon angles and modifications of energies in transforming between the two rest frames of the interacting particles. For normal $e-p$ bremsstrahlung, the differential cross-section is the ultra-relativistic specialization of the Bethe-Heitler formula (e.g. see Jauch and Rohrlich 1980), obtained in the Born approximation:

$$\left.\frac{d\sigma}{d\omega}\right|_{\mathrm{BH}} = 4\,Z^2\,\frac{\alpha_{\mathrm{f}}\,r_0^2}{\omega}\left\{1+\left(\frac{\gamma-\omega}{\gamma}\right)^2-\frac{2}{3}\,\frac{\gamma-\omega}{\gamma}\right\}\left(\log_e\frac{2\gamma(\gamma-\omega)}{\omega}-\frac{1}{2}\right) \quad , \quad \gamma \gg 1 \ , \tag{14}$$

and is not subject to significant Coulomb corrections. Here, γ is the electron Lorentz factor. This formula can be used to compute contributions to the bremsstrahlung spectrum from mildly relativistic energies upwards. The review paper of Blumenthal and Gould (1970) provides a useful and enlightening discussion of various features and issues of bremsstrahlung from ultra-relativistic particles. From Equation (2), assuming a non-relativistic thermal speed $c\beta_{\mathrm{T},s}$ for a species s, the Lorentz factor distribution is easily deduced to be

$$n_s(\gamma) = \frac{n_s\epsilon_s}{(\beta_{\mathrm{T},s})^{1-\Gamma_s}}\,\frac{3(\Gamma_s-1)}{\Gamma_s-1+3\epsilon_s}\,\gamma^{-\Gamma_s} \ . \tag{15}$$

This can be readily folded with the differential cross-section in Equation (14) via an adaption of Equation (1) to yield an emissivity appropriate to the gamma-ray band:

$$\left.\frac{dn_\gamma(\omega)}{dt}\right|_{\mathrm{brems}} \approx \frac{12\Lambda\,\epsilon_e}{(\beta_{\mathrm{T},e})^{1-\Gamma_e}}\,\frac{\Gamma_e-1}{\Gamma_e-1+3\epsilon_e}\,\kappa(\Gamma_e,\,\omega)\,\omega^{-\Gamma_e} \quad , \quad 1 \lesssim \omega \ , \tag{16}$$

where Λ is given by equation (9), and

$$\begin{aligned}\kappa(\alpha,\,\omega) &\equiv \int_1^\infty \frac{dt}{t^\alpha}\left(\frac{4}{3}-\frac{4}{3t}+\frac{1}{t^2}\right)\left[\log_e[2\omega t(t-1)]-\frac{1}{2}\right] \\ &= \frac{3\alpha^2+\alpha+4}{3(\alpha+1)\alpha(\alpha-1)}\left[\log_e 2\omega-\frac{1}{2}-\mathcal{C}\right]+\frac{3\alpha^4+2\alpha^3+15\alpha^2-4}{3(\alpha+1)^2\alpha^2(\alpha-1)^2} \\ &\quad -\left(\frac{4}{3}\frac{\psi(\alpha-1)}{\alpha-1}-\frac{4}{3}\frac{\psi(\alpha)}{\alpha}+\frac{\psi(\alpha+1)}{\alpha+1}\right) \ ,\end{aligned} \tag{17}$$

where $\psi(x) = d[\log_e\Gamma(x)]/dx$ is the logarithmic derivative of the Gamma function, and $\mathcal{C} = \psi(1) = 0.577215\ldots$ is Euler's constant. The evaluation of the integral is facilitated by identity 4.253.6 of Gradshteyn and Ryzhik (1980). The $\omega \sim 1$ values of Equations (8) and (16) are clearly of comparable magnitude. Note also that the bremsstrahlung emissivity traces the electron energy distribution in the relativistic limit. A simple derivation of the form of Eq. (16) is provided in the Appendix.

Determining the emissivity for inverse bremsstrahlung in the limit of ultra-relativistic ions is, in principal, more involved, largely because there are no published expressions for the differential cross-section, integrated over the various interaction angles, that are general enough to take the place of the Bethe-Heitler formula. Exact numerical computations in the Born approximation are presented by Haug (1972). Simple analytic formulae for the cross-section were obtained by Jones (1971), who used the well-known Weizsäcker-Williams method (Weizsäcker 1934; Williams 1935) where the process is treated as stationary electrons Compton scattering the virtual photons carried by the proton's electromagnetic field. Such a technique is quite applicable to hard X-ray and soft gamma-ray energies, but becomes erroneous when $\omega \gg 1$ since then the approximation of the Coulomb potential of the proton by a Fourier decomposition into plane waves (i.e. mimicking free photons) breaks down. Notwithstanding, the approximate formulae of Jones (1971) suffice for the purposes of this analysis (as will become evident shortly); the $\omega \ll 1$ limit of his Equation (4) is

$$\left.\frac{d\sigma}{d\omega}\right|_{\mathrm{IB\text{-}WW}} = \frac{16}{3}\,Z^2\,\frac{\alpha_{\mathrm{f}}\,r_0^2}{\omega}\,\log_e\frac{0.68\gamma}{\omega} \quad , \quad \gamma \gg 1 \quad , \quad \omega \ll 1 \ , \tag{18}$$

where we have included an extra factor of Z^2 to include consideration of ions other than protons. At photon energies $1 \lesssim \omega \ll \gamma$, the numerical computations in Haug (1972) indicate that the differential cross-section approximates a ω^{-2} power-law (exceeding the analytic approximation of Jones 1971), before rolling over near the kinematic maximum energy of $\omega \sim \gamma$. Equation (18) is readily integrated over the power-law Lorentz factor distribution for ions that can be obtained from Equation (15):

$$\left.\frac{dn_\gamma(\omega)}{dt}\right|_{\substack{\rm inv\\ \rm brems}} \approx \frac{16\Lambda\,\epsilon_p}{(\beta_{{\rm T},p})^{1-\Gamma_p}}\,\frac{\Gamma_p-1}{\Gamma_p-1+3\epsilon_p}\,\rho(\Gamma_p)\,\omega^{-\Gamma_p} \quad , \quad \omega \lesssim 1\,, \tag{19}$$

where

$$\rho(\alpha) \;=\; \int_1^\infty \frac{dt}{t^\alpha}\log_e(0.68t) \;=\; \frac{\log_e 0.68}{\alpha-1} + \frac{1}{(\alpha-1)^2}\;. \tag{20}$$

This approximation to the contribution to the inverse bremsstrahlung emissivity from relativistic ions is still correct, up to a factor of order unity, when $\omega \sim 1$, and hence the specification of the range $\omega \lesssim 1$ in Equation (19). When $\omega \gtrsim 1$, the spectrum breaks to assume a $\omega^{-(1+\Gamma_p)}$ form, so that the inverse bremsstrahlung spectrum is steeper than its bremsstrahlung counterpart by an index of roughly unity. We note that while the emissivity in Equation (19) can formally exceed that in Equation (11), in practice this never arises due to the distribution index Γ_p exceeding 2 considerably at near-thermal energies, while $\Gamma_p \lesssim 2$ at relativistic energies. Hence, Equation (11) should be regarded as the appropriate form for optical and X-ray energies. A comparison of Equations (16) and (19) again yields the result that the factor $[\epsilon_p/\epsilon_e]\,(\beta_{{\rm T},p}/\beta_{{\rm T},e})^{\Gamma_p-1}$ roughly defines the ratio of inverse bremsstrahlung to bremsstrahlung emissivities at soft gamma-ray energies.

It is also pertinent to briefly mention electron-electron bremsstrahlung. Since this process is a quadrupole interaction in a classical description, it is strongly suppressed for non-relativistic impact speeds relative to electron-ion bremsstrahlung. This is borne out in the differential cross-sections derived by Fedyushin (1952) and Garibyan (1953), which are of the order of $d\sigma/d\omega \sim 4\alpha_{\rm f} r_0^2/(15\omega)$ (see, for example, the exposition in the Appendix of Baring et al. 1999), a factor of β^2 smaller than the result in Equation (4). However, the $e-e$ bremsstrahlung cross-section for ultra-relativistic impact speeds is necessarily comparable to that for $e-p$ bremsstrahlung (i.e. Equation [14]), as is indicated in the work of Baier, Fadin & Khoze (1967; see also the Appendix of Baring et al. 1999, and the discussion in Blumenthal & Gould 1970), who derived limiting forms using the Weizsäcker-Williams method. The similarity of cross-sections for $\gamma \gg 1$ implies that the ratio of electron-electron bremsstrahlung to electron-proton bremsstrahlung is of the order of unity for plasmas with fairly normal ionic abundances, a fact that was noted by Baring et al. (1999). Hence, $e-e$ bremsstrahlung can play an influential role in the determination of the importance of inverse bremsstrahlung.

2.4. *Expectations for Shock-Heated Environments*

Collecting all the rates so far assembled, it is now a simple enterprise to assert when inverse bremsstrahlung is significant in astrophysical scenarios. Setting $\mathcal{R}_{\rm O-X}$ to be the ratio of Equations (11) to (8) at $\omega \sim (\beta_{{\rm T},e})^2$, so as to represent the ratio of inverse bremsstrahlung to bremsstrahlung at optical to X-ray energies, and $\mathcal{R}_{\rm MeV}$ to be the ratio of Equations (19) to (16) at $\omega \sim 1$, representing the inverse bremsstrahlung/bremsstrahlung ratio at soft gamma-ray energies, we arrive at

$$\mathcal{R}_{\rm O-X} \;\sim\; \frac{\epsilon_p}{\epsilon_e}\left(\frac{m_e}{m_p}\,\frac{T_p}{T_e}\right)^{(\Gamma_p-1)/2} \;\sim\; \mathcal{R}_{\rm MeV}\;, \tag{21}$$

expressing the thermal speeds of the two species in terms of the electron and proton temperatures T_e and T_p. Similar order-of-magnitude estimates for such ratios can be obtained for other ionic species such as He^{2+}. In Equation (21), it must be emphasized that for the optical/X-ray band ratio, the index Γ_p refers to *the mean index ranging from thermal proton speeds up to thermal electron ones*, while for $\mathcal{R}_{\rm MeV}$, Γ_p represents the mean index of protons with $\gamma \gg 1$. Hence, given the general upward curvature of spectra for cosmic rays accelerated in non-linear shocks (e.g. Eichler 1984; Jones & Ellison, 1991), we expect $\Gamma_p > 2$ for the optical/X-ray band considerations and $\Gamma_p \lesssim 2$ for the gamma-ray band. Since the *gamma-ray* spectrum for inverse bremsstrahlung (see the discussion after Equation [19]) is steeper than that for bremsstrahlung in Equation (16), $\mathcal{R}_{\rm MeV}$ defines an upper bound to the ratio of emissivities for the two processes in hard gamma-rays, a bound that is actually conservative given the expectation that $e-e$ bremsstrahlung will amplify the bremsstrahlung signal by a factor of order 2 in the gamma-ray band.

The ratio ϵ_p/ϵ_e of efficiency factors is a free parameter for a shock acceleration model. As noted at the beginning of Section 2, while efficient acceleration of protons is generally expected due to strong turbulence local to the shock (e.g. Ellison, Baring & Jones 1996), so that $\epsilon_p \sim 0.1$, to order of magnitude (which is borne out in observations of interplanetary shocks: see Baring et al. 1997), much less is known about the value of ϵ_e, essentially due to a paucity of *in situ* observations of electron acceleration in the heliosphere. However, this difficulty can be circumvented in part (at least in astrophysical scenarios) by arguing that cosmic ray data are a strong indicator of the acceleration efficiency in typical cosmic ray sources, principally supernova remnant shocks. The electron-to-proton abundance ratio above 1 GeV (where both species are relativistic) is well-known to be of the order of a few percent (e.g. see Müller et al. 1995), which constrains the typical acceleration efficiency, assuming that differences in electron and proton propagation in the interstellar magnetic field at these energies are not great. From the forms in Eq. (2), this ratio can be estimated as a function of the temperatures, masses and spectral indices of the two species. For an isothermal plasma with $\Gamma_e \sim \Gamma_p \sim 2$, one quickly determines that $n_e(1\ {\rm GeV/c})/n_p(\ 1\ {\rm GeV/c}) \sim [\epsilon_p/\epsilon_e]\,(m_e/m_p)^{1/2}$, so that the observed abundance ratio at momenta 1 GeV/c is reproduced only if ϵ_e is of the same order of magnitude as ϵ_p, i.e. injection of electrons into the Fermi mechanism is indeed efficient. Relaxing the isothermal and equal index stipulations yields a range of ϵ_p/ϵ_e on either side of unity.

As will be apparent in the subsequent subsection, a specific simulation of the acceleration mechanism applied to supernova remnants yields values of ϵ_p/ϵ_e not too disparate from unity.

The temperature ratio T_e/T_p clearly controls the importance of inverse bremsstrahlung relative to bremsstrahlung, both through its explicit appearance in Eq. (21), and also via its influence on the efficiency ratio ϵ_p/ϵ_e. In shocked plasmas, this ratio is expected to far exceed m_e/m_p, thereby implying that *inverse bremsstrahlung is insignificant in most astrophysical scenarios involving shocked plasmas*. This is the principal result of this paper; it is contingent upon there being far fewer protons than electrons above electron thermal speeds, an occurrence we believe to be common near astrophysical shocks.

Evidence for this can be derived from both observational and theoretical sources. On the observational side, there is a clear indication of the lack of velocity equipartition in electron and proton populations near the Earth's bow shock. Feldman (1985) exhibits measurements of electron and ion velocity distributions that lead to the identification of (i) strong electron heating during shock passage, and (ii) downstream velocity thermal ratios for electrons to ions (mostly protons) of the order of 50 (i.e. $m_eT_p/m_pT_e \sim 0.02$). The situation for travelling interplanetary shocks is similar. While ion distributions indicate shock heating that couples to the ram pressure differential across such weak shocks (e.g. see Baring et al. 1997 for Ulysses SWICS data, where $T_p \sim 5\times10^5\,\mathrm{K}$), measurements of electron populations are generally sparse. Temperatures of the electron component of the solar wind upstream of interplanetary shocks is typically in the $3\times10^4-2\times10^5\,\mathrm{K}$ range (Hoang et al. 1995), commensurate with large scale solar wind averages (Phillips, et al. 1995), and therefore are a sizeable fraction of the downstream ion velocity dispersion temperatures in the Ulysses data set. Hence, in the absence of any electron heating at the low Mach number interplanetary shocks encountered by Ulysses, $m_eT_p/m_pT_e \sim 10^{-3}-10^{-2}$ will be obtained. Such values are evinced in the ISEE data presented in Feldman (1985), which exhibits only modest heating of electrons by interplanetary shocks.

Outside the heliosphere, the evidence for significant electron heating is sparse and more circumstantial. Shocks at the outer shells of young supernova remnants (SNRs) provide the best indication. These move typically at speeds 500–3000 km/sec, depending on the SNR age and the mass of the progenitor, suggesting ion heating to temperatures of the order of $5\times10^7-2\times10^9\,\mathrm{K}$ per nucleon. Electron temperatures in SNRs can be deduced from observations of thermal X-ray emission (for a recent collection of observational studies, see Zimmermann, Trümper, & Yorke 1996), and are typically $\sim 10^7\,\mathrm{K}$. Therefore, it is expected that $m_eT_p/m_pT_e \sim 5\times10^{-3}-0.2$ in these sources. Inferences of electron to proton temperature ratios in active galactic nuclei are inconclusive, largely due to the absence of a marker for ion temperatures.

The theoretical expectation that $m_eT_p/m_pT_e \ll 1$ is derived from considerations of dissipation in the shock layer. In a diffusive acceleration process where spatial diffusion is effected via *elastic* collisions of particles with magnetic irregularities that are anchored in the background fluid, the acceleration from thermal energies is effectively a velocity-dependent process (e.g. see the reviews of Drury 1983; Jones & Ellison 1991). This situation corresponds to dissipative heating in the shock layer that is independent of mass of the species. Baring et al. (1997) illustrates such a situation in their modelling of accelerated proton and He populations at nearby interplanetary shocks. However, dissipation in the shock layer cannot be entirely elastic in origin in any frame of reference, due in part to the different mobilities of electrons and ions. In a quasi-perpendicular shock, it is clear that the much smaller Larmor radii of electrons (relative to ions) that cross the shock lead to the establishment of induced electric fields via charge separation. In quasi-parallel shocks, similar electric fields exist, due to the turbulence of the field structure in the shock layer. In fact, generalized shock structure including out-of-the plane magnetic field components requires the presence of electric fields in all frames of reference (Jones & Ellison 1987; 1991). Such fields heat the low energy electrons at the expense of the energy of the ions (see the discussion of Jones 1999), and thereby effect at least a partial equilibration in energy, providing significant theoretical support for the contention that $m_eT_p/m_pT_e \ll 1$. In general, a complex array of wave modes and instabilities can precipitate strong acceleration/heating of electrons. Limited evidence for such heating can be found in the hybrid plasma simulations of Cargill and Papadopoulos (1988) for non-relativistic shocks, and the full plasma simulations of Hoshino et al. (1992) for relativistic shocks in a pair-dominated ion-pair plasma. However, these two works do not simultaneously probe fully three-dimensional hydrogenic plasmas with truly realistic ion/electron mass ratios (so as to address a full array of wave modes). Three-dimensional simulations are required to accurately account for particle diffusion in all directions (e.g. see the discussion in Jones, Jokipii & Baring 1998). Hence, a definitive simulational assessment of the degree of electron heating in shocked plasmas remains an outstanding problem.

2.5. *A Simulational Illustration*

The expected dominance of bremsstrahlung can be illustrated using model predictions from a Monte Carlo simulation of diffusive acceleration in non-relativistic shocks. The Monte Carlo technique used to model diffusive shock acceleration is well-documented in the literature (e.g. see Jones & Ellison 1991; Baring, Ellison, & Jones 1993; Ellison, Baring, & Jones 1996; and more recently, Baring et al. 1999, for a description of electron injection). It is a kinematic model, closely following Bell's (1978) approach to diffusive acceleration, where the simulation is used to calculate, in effect, solutions to a Boltzmann equation for particle transport involving a collision operator, without making any assumption concerning the isotropy of particle distributions. Particles are injected at a position far upstream and allowed to convect into the (infinite plane, steady-state) shock, diffusing between postulated scattering centers (presumably magnetic irregularities in the background plasma and self-generated turbulence) along the way. As particles diffuse between the upstream and downstream regions, they continually gain energy in accord with the Fermi mechanism. Particle splitting is used very effectively to maintain excellent statistics over a large dynamic range. The approach adopts a phenomenological mean free path, $\lambda_i \propto r_{\rm g}^{\alpha}$ (with $\alpha \sim 1$ for all ions and energetic electrons; for near-thermal electrons, see Baring et al. 1999 for details) to encompass the complications of plasma microphysics, where $r_{\rm g} = pc/(ZeB)$ is the particle gyroradius. The aptness of this power-law prescription to shocked plasma environments is supported by particle observations at low energies at the Earth's bow shock, Ellison, Möbius, & Paschmann 1990), deductions from ions accelerated in solar particle events (Mason, Gloeckler, & Hovestadt 1983), and also from plasma simulations (Giacalone, Burgess & Schwartz 1992). Furthermore, in the strong field turbulence expected (and seen) at shocks, near-Bohm diffusion, $\lambda_i \gtrsim r_{\rm g}$, imposes an $\alpha \sim 1$ requirement.

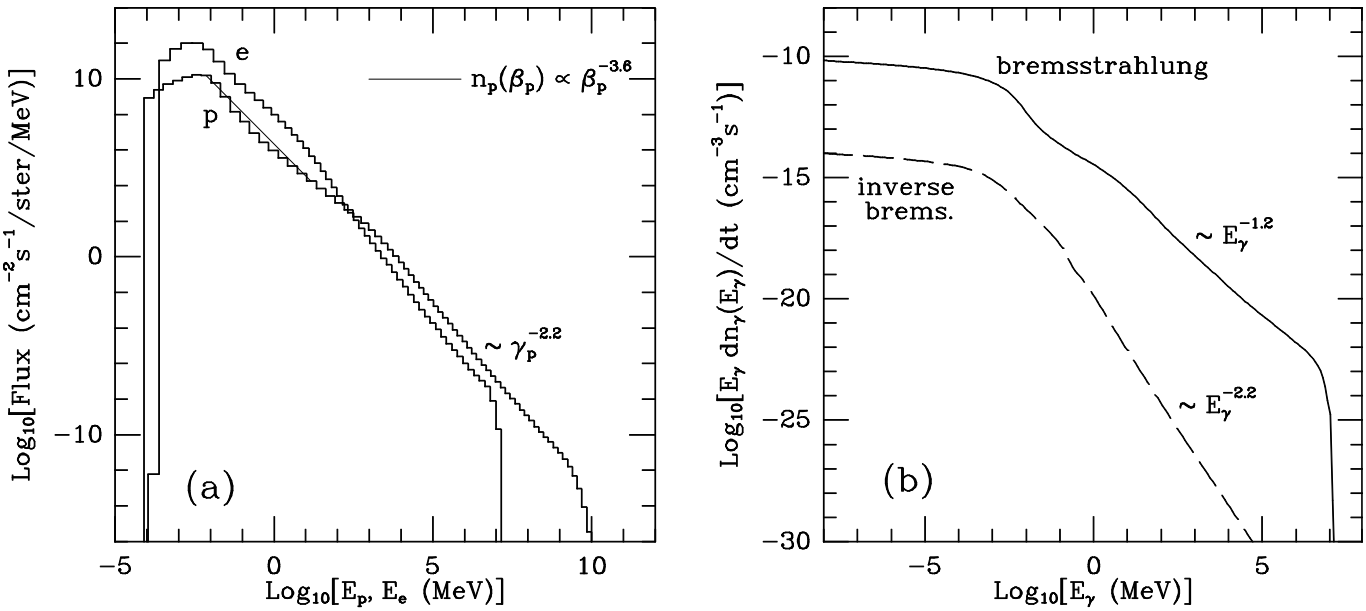

FIG. 1.— Accelerated particle distributions (a) from a Monte Carlo simulation of acceleration at steady-state cosmic-ray modified non-relativistic shocks, specifically from the modelling by Ellison, Goret & Baring (1999) of broad-band spectra for the supernova remnant Cas A, together with (b) the bremsstrahlung and inverse bremsstrahlung emissivities resulting from these distributions. The electron and proton distributions are omni-directional fluxes, binned in kinetic energy intervals, in accord with our previous expositions, and represent the differential energy distributions multiplied by the particle speed; they were obtained for a shock speed of 2800 km/sec and an ISM density of $3\,\mathrm{cm}^{-3}$. An approximate power-law velocity distribution with index $\Gamma_p = 3.6$ is depicted to facilitate the discussion in the text. The photon emissivities are multiplied by photon energy, i.e., E_γ times the differential spectrum.

Typical predictions for the proton and electron distributions (downstream of a shock) using the Monte Carlo technique are depicted in Figure 1, taken from the Ellison, Goret & Baring's (1999) study of shock acceleration in the supernova remnant Cas A (similar spectra are presented in Baring et al. 1999). The distributions are exhibited as omni-directional fluxes (i.e. differential energy fluxes multiplied by particle velocity: $v\,dn/dE \equiv c\beta n(E)$), mimicking the spectra measured by particle detectors in the heliosphere. Hence, for non-relativistic speeds, the momentum (or velocity) distribution index Γ_s is exactly twice the slope of the curves in Figure 1a, while for ultra-relativistic particles, Γ_s is identical to the depicted slopes, which for both the electrons and protons is roughly $\Gamma_e \approx \Gamma_p \approx 2.2$. The particular simulation output that is illustrated possesses a hot electron component in the downstream plasma, with a temperature roughly half that of the protons. The light power-law drawn in Figure 1a, with a velocity distribution as labelled, approximates the proton distribution between thermal proton and thermal electron speeds; it has an index of $\Gamma_p \approx 3.6$ (i.e. flux distribution $\beta_p n_p(E_p) \propto E_p^{-1.8}$). Observe that the Monte Carlo curves are not pure power-laws in momentum but exhibit a slight upward curvature in the relativistic portions of the distributions (and also significant curvature at suprathermal non-relativistic energies for the protons), a central feature of the non-linear feedback between the ion diffusion and the shock hydrodynamics in cosmic-ray modified shocks that is well-documented (e.g. Eichler 1984; Ellison & Eichler 1984; Jones & Ellison 1991; Ellison, Jones & Baring 1996). Because such hydrodynamics is strongly regulated by the feedback between particle acceleration and escape from the remnant, the generated proton distributions are not very sensitive to the prescription of λ as a function of rigidity.

Electrons, on the other hand, are dynamically unimportant, so that their spectral normalization (but not spectral shape) is sensitive only to their injection efficiency, which couples to the electron-to-proton temperature ratio. While this is somewhat uncertain, we used reasonable shock speeds and observed X-ray temperatures from remnants (e.g. Zimmermann, Trümper, & Yorke 1996) to adopt appropriate values. Note also that the ratio of the electron to proton populations in the 1–10 GeV range (contingent upon the assumed injection efficiency) for the specific results in Figure 1a varies between 15% and 5%, somewhat larger than observed e/p cosmic ray ratio in this energy range (e.g. see Müller et al. 1995); e/p ratios more consistent with the cosmic ray data are readily obtained (Baring et al. 1999) by the Monte Carlo simulation.

Figure 1b depicts the emissivities for bremsstrahlung (solid curve) and inverse bremsstrahlung (dashed curve) that result from the particle distributions in Figure 1a. The flat spectra below X-ray energies correspond to $dn_\gamma(\omega)/dt \propto \omega^{-1}$, approximating the low energy results in Equations (8) and (11), and interestingly, close to the index observed in the cosmic X-ray background below 10 keV (thus motivating the application discussed in Boldt & Serlemitsos 1969). Above the electron thermal energy, the spectra steepen for both processes, and in the gamma-ray regime, the inverse bremsstrahlung spectrum ($\propto \omega^{-3.2} \approx \omega^{-(1+\Gamma_p)}$) is steeper than that of bremsstrahlung ($\propto \omega^{-2.2} \approx \omega^{-\Gamma_e}$), in accord with Equation (16) and the discussion following Equation (19).

We note that the steep shoulder in the bremsstrahlung spectrum in the X-ray band defining the roll-off above the thermal emission could potentially provide an alternative explanation (Baring et al. 1999) to synchrotron emission for the non-thermal X-rays seen in the supernova remnants SN 1006 (Koyama et al. 1995), IC 443 (Keohane et al. 1997) and Cas A (Allen et al. 1997). The illustrated case, of index ~ 2.8 for just over half a decade in energy, lies in between the index of ~ 2.3 ASCA obtained for IC 443 and the X-ray observations of Cas A and SN1006 (~ 3). While this issue is discussed in more detail in Ellison, Goret & Baring (1999), it

is important to remark that inferences of the spectral index of a non-thermal component in X-ray data are very sensitive to the choice of temperature of a thermal component and the shape of a non-thermal continuum. Restrictions to pure power-laws for the continuum, while convenient, are not really appropriate for either synchrotron radiation turnovers or bremsstrahlung emission mechanisms, so that conclusions about the physical mechanism in operation should be guarded. For example, the RXTE data in Allen et al. (1997) on Cas A suggests a spectral break at $16\,\mathrm{keV}$, steepening from an index ~ 1.8 to one of ~ 3.0, data that at first sight does not appear inconsistent with a bremsstrahlung model in the transition region from thermal to non-thermal energies (though probably with a slightly higher temperature than the case depicted in Figure 1). The critical distinction between synchrotron turnover and "transition" bremsstrahlung models therefore lies in the expected flattening above the transition region in the bremsstrahlung spectrum (e.g. see Figure 1b). This provides an observational discriminant via broader-band observations beyond the scope of ASCA and RXTE, though current instrumental sensitivities (such as those of XMM and Integral) are probably insufficient to answer this question. A related situation arises with diffuse/unresolved emission in the galactic ridge, and recent broad-band X-ray spectra of the Scutum arm (Valinia, Kinzer & Marshall 1999) suggest a turnover in the 50–100 keV range, which could indicate the superposition of Comptonized (or synchrotron) emission from unresolved discrete sources. However, we note that data statistics in the OSSE band are not sufficient to preclude a flattening at higher energies that would be characteristic of bremsstrahlung of either discrete source or diffuse origin.

Returning to the issue at hand, the particular example in Figure 1 gives a strong dominance of bremsstrahlung over inverse bremsstrahlung. In fact, given the $\Gamma_p \approx 3.6$ index for non-relativistic speeds, and $T_e/T_p \sim 1/2$, Equation (21) can be simply applied to estimate a ratio of ~ 8000 between the two processes (for $\epsilon_p/\epsilon_e = 1$), close to the ratio deduced in the optical band from Figure 1b. This agreement highlights the viability and usefulness of the schematic distributions in Eq. (2), and also that of the consequent quantitative estimates of the various emissivities throughout this paper. Observe that the only way to increase $\mathcal{R}_{\mathrm{O-X}}$ is to dramatically lower the temperature of the electrons relative to the protons, but to do so would cause a corresponding decrease in the e/p ratio at relativistic energies (and influence the ratio ϵ_p/ϵ_e of injection efficiencies), well below observed values in the 10 GeV band (see, e.g. Müller et al. 1995, for a recent compendium of data). As argued above, it is unlikely that $\mathcal{R}_{\mathrm{O-X}} \gtrsim 0.01$ will be realized often in shocked astrophysical plasmas.

It is natural to question whether such a result holds for ions heavier than protons. Clearly, both the bremsstrahlung and inverse bremsstrahlung contributions from helium and heavier elements are given by their abundance (usually small) multiplied by Z^2. The Z^2 enhancement provides significant bremsstrahlung emissivities when helium targets (typically of $\sim 5\%$ abundance) are involved. For inverse bremsstrahlung, the Z^2 amplification potentially could be offset by a more severe mass ratio reduction, if lower thermal speeds are precipitated downstream of shocks. There is little or no evidence for such lower thermal speeds for ions heavier than protons. In fact, the Ulysses SWICS data on the 91097 interplanetary shock unequivocally indicates the contrary: the shock dissipation mechanism generates virtually identical velocity dispersions for both protons and alpha particles (Baring, et al. 1997). Such a property is well-modelled by the Monte Carlo technique, since the elastic scattering hypothesis that it employs renders the shock acceleration model a velocity-dependent injector. This scattering assumption, together with a rigidity-dependent diffusion coefficient, is rigorously put to the test in the successful prediction (Meyer, Drury, & Ellison 1997; Ellison, Drury, & Meyer 1997) of abundances of ions of various metallicities in the cosmic ray population, using a supernova remnant site for the acceleration of dust grains. These pieces of evidence point to an approximate velocity equipartition of thermal ions in shocks, so that the criterion in Equation (21) renders the conclusion that inverse bremsstrahlung is generally insignificant in shocked astrophysical plasmas also applicable to contributions from ions heavier than protons.

3. DISCUSSION

The unimportance of inverse bremsstrahlung for shocked environs in discrete sources, the principal result of this paper, can be interpreted in the broader context of invocations of inverse bremsstrahlung in diffuse emission problems. The pre-eminent implication of this result is obviously that supernova remnants will dominate their environs in X-ray and gamma-ray luminosity, and therefore will obscure truly diffuse emission components in extended regions such as the galactic ridge and the Orion complex, if the source remnants are too densely clustered. Hence, it is of significant interest to identify the length scales on which discrete sources such as supernova remnants provide a dominant contribution to unresolved X-ray and gamma-ray emission in the galaxy, as a guide to modelers and also to aid the interpretation of experimental results.

The discussion of this issue is not restricted to just the ratio of bremsstrahlung from cosmic ray primary (i.e. shock-accelerated) electrons and inverse bremsstrahlung from cosmic ray ions. The works of Tatischeff, Ramaty & Kozlovsky (1998) and Dogiel et al. (1998) argued that suprathermal proton bremsstrahlung emission levels are comparable to those of bremsstrahlung from knock-on electrons in the Orion complex, given the then (and now defunct) Comptel nuclear line detection in this region. Knock-on electrons are generated from the cool ambient interstellar population via Coulomb collisions with energetic cosmic ray ions (and perhaps electrons). Since the stopping length (on ambient electrons *or* protons) for 25 keV electrons in interstellar environments of typical density is of the order of 100 pc (e.g. see Valinia & Marshall 1998), Coulomb collisions are clearly relevant for electrons in large scale systems such as the Orion cloud complex. Coulomb scattering simultaneously mediates both energization of ambient electrons and cooling of cosmic ray primary electrons. In contrast, shocked astrophysical plasmas such as those in young to middle-aged supernova remnants are collisionless, so that knock-on populations are locally negligible. Given the conclusions of this paper relating to shock-heated plasmas, it is salient to also examine when knock-on electron bremsstrahlung is a significant contributor to diffuse/unresolved emission relative to primary electron bremsstrahlung. Note that the comparisons of Tatischeff, Ramaty & Kozlovsky (1998) and Dogiel et al. (1998) of inverse bremsstrahlung relative to knock-on electron bremsstrahlung did not include an abundant, shock-accelerated electron population, and therefore did not address this issue.

3.1. *Knock-on Electrons*

First, we address the question of whether knock-on electrons are abundant relative to cosmic ray primary electrons. For mono-energetic cosmic rays, non-relativistic knock-on electrons possess an E^{-2} kinetic energy distribution regardless of whether the energetic cosmic rays are ions (e.g. see Hayakawa 1969) or electrons (Gould 1972; true also for relativistic electrons: see Baring 1991), which corresponds to a β^{-3} velocity distribution. This is comparable in steepness to the shock-accelerated electron distribution exhibited in Fig. 1a. However, in spite of the ambient (and therefore also knock-on) electrons being much more abundant than cosmic ray ones, the relative population level at almost relativistic speeds defines the criterion for the importance of knock-on electrons in producing X-ray bremsstrahlung. The knock-on electron population extends upward from extremely low thermal energies (temperatures of 3–100 K; see Dogiel et al. 1998 for a listing of parameters for the Orion complex). Assuming that only a minority of ambient electrons can be energized in knock-on collisions without disturbing the thermal balance of the ambient interstellar medium, it is straightforward to determine that the distribution $n_e(E_{\rm MeV}) \sim 10^{-9} n_e\, T_1\, E_{\rm MeV}^{-2}$ MeV^{-1} cm^{-3} forms a conservative upper bound to the knock-on energy distribution out to MeV energies. Here T_1 is the ISM temperature in units of 10 K, and n_e is the ISM density in units of cm^{-3}, typically of the order of 1 cm^{-3} in the normal ISM, and ~ 100 cm^{-3} in dense interstellar regions. Also, $E_{\rm MeV}$ is the electron energy in units of MeV.

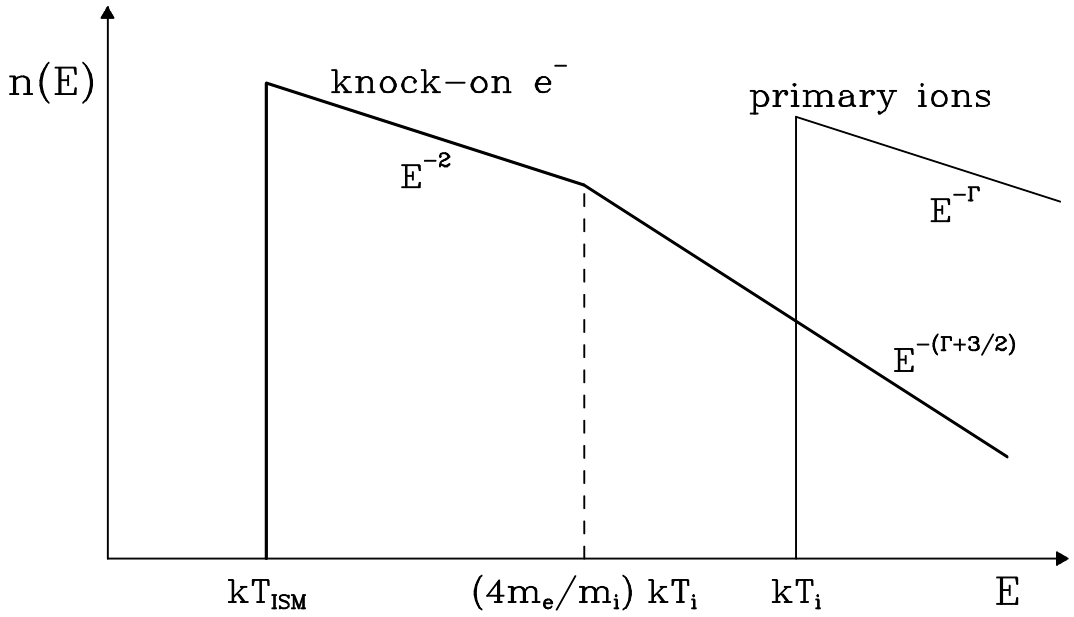

FIG. 2.— A schematic depiction of the knock-on electron distribution (heavy line) generated by a cosmic ray ion distribution that is a power-law above thermal energies represented by a non-relativistic temperature T_i ($\ll m_i c^2/k$). For ions originating in SNRs, typically $kT_i \sim 10^{-2} - 1$ MeV from shock heating. The knock-on distribution extends upwards from the temperature $T_{\rm ISM}$ of the ambient ISM, and steepens above the kinematic break at twice the cosmic ray ion thermal speed (i.e. $E \sim (4m_e/m_i)kT_i$; see Baring 1991, for example, for a discussion of kinematics). While knock-on electrons may dominate cosmic ray primaries by number, they suffer a substantial paucity at high energies.

This upper bound is actually a gross overestimate, given that it corresponds to 100% of the ambient electron population being energized. Furthermore, due to the kinematic maxima for the energies imparted to cold electrons by Coulomb collisions, above the thermal speed of the ballistic cosmic rays, which for ionic projectiles is unlikely to exceed typical shock speeds for supernova remnants of a 500-3000 km/sec, the knock-on spectrum steepens from the dependence E^{-2}. The knock-on distribution can then be shown to roughly follow an $E^{-3/2-\Gamma_p}$ distribution for a cosmic ray ion spectrum $\propto E^{-\Gamma_p}$ (derivable, for example, using Eq. (9) of Baring 1991), rendering the knock-on electron population at around 100 keV far smaller than the above bound; see Figure 2 for a schematic depiction. An approximate refined estimate for the knock-on distribution would then be $n_e(E_{\rm MeV}) \sim 0.1 n_e\, T_1\, [E_{\rm MeV}/10^{-4}]^{-3/2-\Gamma_p}$ MeV^{-1} cm^{-3} for $E_{\rm MeV} \gtrsim 10^{-4}$. This can be compared with a rough estimate for the non-thermal electron distribution expected for efficient acceleration at a remnant's shock: $n_e(E_{\rm MeV}) \sim 10^5 n_e\, T_7\, [E_{\rm MeV}/10^{-4}]^{-2}$ MeV^{-1} cm^{-3}, where here T_7 is the shocked plasma temperature in units of 10^7 K. Since $T_7 \sim 1$ near SNR shocks, clearly the primary cosmic ray source spectrum locally swamps the knock-on one. Away from such shocks, diffusion dilutes the primary source spectrum down to cosmic ray flux levels.

While a specific prediction for the ambient cosmic ray primary electron density could be made via a particular acceleration model (such as the Monte Carlo technique used above), combined with a specific diffusive propagation model, we prefer to make use of existing experimental cosmic ray data under the premise that dense interstellar regions are not extraordinarily peculiar in their cosmic ray properties. Müller et al. (1995; see also Müller & Tang 1987) exhibit the primary electron flux at Earth above around 3 GeV. From their data, one quickly arrives at the differential energy distribution for electrons of $n_e(E_{\rm MeV}) \sim 10^{-4}\, E_{\rm MeV}^{-3.25}$ MeV^{-1} cm^{-3} at energies above 3 GeV. Direct extrapolation of this down to 100 keV (i.e. well-below energies where heliospheric modulation impacts measurements of the cosmic ray spectrum) would lead to the conclusion that cosmic ray electrons should dominate the maximum possible density of knock-on electrons by around 4 orders of magnitude, and the refined estimate above of the knock-on density by

a factor of 10^9 or more (for $\Gamma_p \gtrsim 2$), for realistic values of the ISM temperature T_1. However, the primary electron spectrum is probably much flatter in the 100 keV to 3 GeV band than measured at higher energies. The diffuse radio synchrotron emission in the 30–600 MHz band ($\propto \nu^{-2/3}$) in our galaxy suggests (e.g. see the review by Webber 1997) a cosmic ray electron distribution $\propto E^{-7/3}$ between 500 MeV and 2.2 GeV. This flattening probably reflects the transition from directly sampling contributions to the cosmic ray spectrum near discrete sources (which generally should possess flatter $\sim E^{-2}$ distributions like those in Figure 1) to larger-scale steepening imposed by cosmic ray propagation effects. Even using an extrapolation $n_e(E_{\rm MeV}) \sim 10^{-6}\, E_{\rm MeV}^{-2.67}$ MeV^{-1} cm^{-3} at energies below 300 MeV based on the inferences from the radio data, one arrives at the conclusion that the cosmic ray primary electron population would far exceed any knock-on component generated by cosmic ray ions.

3.2. *Diffuse and Unresolved Emission*

Hence, it follows that a knock-on population of electrons can only generate a significant amount of electron bremsstrahlung emission in dense interstellar regions provided that there is a profound paucity of cosmic ray electrons in the 30 keV–1 MeV range. Cooling of electrons through Coulomb and ionization losses potentially can create such a paucity; lower energy electrons cool faster than more energetic ones do. Therefore, a depletion of cosmic ray electrons below 1 MeV is a distinct possibility on scales considerably greater than 10pc outside the supernova remnants that act as sources of cosmic rays. Specifically, using the numbers quoted by Valinia and Marshall (1998), 25 keV electrons that would emit bremsstrahlung in the RXTE band have a collisional loss pathlength of around 100pc in the ISM. This linear scale $\lambda_{\rm Coul}$ can be translated into a radial scale $r_{\rm Coul}$ by incorporating the effects of diffusion due to the turbulent interstellar field. The mean free path $\lambda_{\rm B}$ for such diffusion is extremely uncertain, but as is the case for the undisturbed interplanetary medium in the heliosphere, estimates for $\lambda_{\rm B}$ (by coupling to the field irregularity scale; e.g. see Kim, Kronberg & Landecker 1988) far exceed particle gyroradii, at around 100pc. This implies that for 25 keV electrons, $r_{\rm Coul} = [\lambda_{\rm Coul}\, \lambda_{\rm B}]^{1/2} \sim 100\,{\rm pc}$ defines the maximal extent of their "Coulomb halo" around a SNR. For higher energy electrons, the radius of this halo is larger, so that at any given radius, the primary electron spectrum is depleted up to the energy at which Coulomb losses become insignificant.

Irrespective of whether and on what scales such depletions exist (no data pertaining to cosmic ray electrons samples this energy range), the dominance of bremsstrahlung from primary cosmic ray electrons over inverse bremsstrahlung from primary cosmic ray protons that is established in this paper would lead to the major contribution to unresolved "diffuse" X-ray emission in Orion or the galactic ridge coming from discrete sources, unless the volume filling factor of supernova remnants in the interstellar medium is less than 10^{-4}–10^{-3}. While accurate determination of this factor is difficult, extant compendia of supernova remnants (e.g. Helfand et al. 1989; Green, 1999) lead to estimates at the lower end of this range (i.e. $\sim 10^{-4}$), to order of magnitude. Hence, while it is possible that such conditions might prevail in some galactic interstellar environments, and more probably at moderate latitudes above the disk, we contend that primary cosmic ray electron bremsstrahlung will simultaneously dominate bremsstrahlung from secondary knock-on electrons and inverse bremsstrahlung mediated by cosmic ray ions as contributors to diffuse X-ray emission in the most important and interesting environments.

When this is not the case, primary electron bremsstrahlung signals (of spectral index 2–3) will be confined to discrete source locales of scales $\sim$ 10–100pc, i.e. near supernova remnants, while suprathermal proton bremsstrahlung and knock-on electron bremsstrahlung (of similar spectral indices) will sample the length scales appropriate to ionic collisional losses, namely $\sim 0.2\,{\rm Mpc}$ for the 50MeV protons that can generate inverse bremsstrahlung X-rays in the RXTE band. To reiterate, these length scales will be appropriately contracted in linear dimensions if they exceed the diffusive scales for such particles in the interstellar magnetic field (e.g. to $\sim 5\,{\rm kpc}$ from the protons: see Valinia and Marshall 1998). Such radiation "clumping" issues should form a focus of discussions of diffuse and unresolved emissions. Note that because $\sim 50\,{\rm MeV}$ cosmic ray protons are not easily depleted on scales $\ll 5\,{\rm kpc}$, and since the low ISM temperature forces the knock-on distribution to low levels, we expect that generally inverse bremsstrahlung dominates knock-on electron bremsstrahlung outside remnants.

An observationally interesting question concerns how easily bremsstrahlung signals from primary cosmic ray electrons associated with SNRs can by distinguished from truly compact sources such as neutron stars or black holes, given current angular resolution capabilities of X-ray telescopes. Spectral signatures may provide the answer prior to improvements in instrumental resolving power. The similarity of unresolved emission spectra in source-rich and source-poor galactic regions (ASCA data: Tanaka, Miyaji & Hasinger 1999), and the spectral similitude of observations of the Scutum arm (RXTE/OSSE data: Valinia, Kinzer & Marshall 1999) and galactic X-ray binaries and black hole candidates provide clues impinging upon this issue.

Observe also that the expected general dominance of bremsstrahlung from primary electrons returns one to the energetics issues raised by Skibo, Ramaty & Purcell (1996), who discerned that the general inefficiency of bremsstrahlung processes in the X-ray band relative to collisional and ionization losses elicits difficulties in generating the requisite luminosity. In passing, we note that clumping of emission in the proximity of remnants will help alleviate the energy supply problem for a bremsstrahlung origin of the galactic diffuse X-ray emission, by diminishing such losses for the electrons.

4. CONCLUSION

In conclusion, the results of this paper indicate that inverse bremsstrahlung in the optical to X-ray and gamma-ray bands can be safely neglected in most models of discrete sources invoking shock acceleration. This follows from the approximate ratio, posited in Equation (21), of inverse bremsstrahlung to bremsstrahlung from primary non-thermal electrons, together with expectations for dissipational heating of electrons in the shock layer. Both observational and theoretical evidence favors electron temperatures almost comparable to, and certainly not very deficient relative to, proton temperatures in shocked plasmas. Hence shocked environments in discrete sources such as supernova remnants should have inverse bremsstrahlung contributing only in a minor capacity to the overall emission, a situation that could apply also to larger, extended interstellar regions such as the galactic ridge, provided that

the volume filling factor associated with remnants exceeds around $10^{-4}-10^{-3}$. Since this filling factor may sometimes be lower, perhaps at moderate to high galactic latitudes, we find that in such cases, inverse bremsstrahlung can contribute significantly in the X-ray band on length scales of the order of 50–100pc or greater, thereby posing an interesting observational goal to resolve bright bremsstrahlung X-ray emission concentrated around discrete sources from any truly diffuse inverse bremsstrahlung component that spatially traces the cosmic ray ion population. We also contend that bremsstrahlung from knock-on electrons is probably always a minor contribution, and find that the dominance of bremsstrahlung from primary cosmic ray electrons over inverse bremsstrahlung in the vicinity of remnants is even more enhanced in the gamma-ray band.

We thank Stephen Reynolds, Elihu Boldt, Azita Valinia and Peter Serlemitsos for discussions, Vincent Tatischeff and the anonymous referee for comments helpful to the improvement of the presentation, and Bob Gould for pointing out certain literature on bremsstrahlung to us.

APPENDIX

In this brief Appendix, a pedagogical alternative to the derivation of the various bremsstrahlung emissivities is provided, using approximate, simplified cross-sections, so as to elucidate the results obtained in the text by diminishing the mathematical complexity. To this end, the expressions obtained here are proportionalities, possessing only the principal variables. Eqs. (1) and (2) are again the starting points. Instead of using Eqs. (4) and (14) for the non-relativistic and ultrarelativistic bremsstrahling differential cross-sections, it is expedient to use a single approximation

$$\left.\frac{d\sigma}{d\omega}\right|_{\text{NR-ER}} \sim \frac{16}{3}\,Z^2\,\frac{\alpha_{\rm f}\,r_0^2}{\omega}\,\frac{1}{\beta^2}\,\Theta\Big(\frac{\omega}{\gamma-1}\Big) \quad , \tag{A1}$$

where $\Theta(x)$ is a step function that is unity for $0<x<1$, and zero otherwise. Consider first normal bremsstrahlung. The integrations over the electron distribution are straightforward, with both the $p\le p_{{\rm T},e}$ and $p>p_{{\rm T},e}$ portions contributing for $\omega\lesssim\beta_{{\rm T},e}^2\ll 1$, and just the high momentum tail being sampled for $\beta_{{\rm T},e}^2\ll\omega\ll 1$. The resulting proportionalities can then be summarized as (for $\Lambda=Z^2n_pn_e\alpha_{\rm f}r_0^2c$)

$$\left.\frac{dn_\gamma(\omega)}{dt}\right|_{\rm brems} \propto \frac{\Lambda}{\beta_{{\rm T},e}}\begin{cases}\dfrac{1}{\omega}\left(\dfrac{1}{2}+\dfrac{\epsilon_e}{\Gamma_e}\right), & \omega\lesssim\beta_{{\rm T},e}^2\ll 1,\\[2ex] \epsilon_e\,\dfrac{\beta_{{\rm T},e}^{\Gamma_e}}{\omega^{1+\Gamma_e/2}}\ , & \beta_{{\rm T},e}^2\ll\omega\ll 1,\end{cases} \tag{A2}$$

dependences that are clearly evident in Eq. (8); the absence of logarithmic factors is an obvious consequence of the simplification of the cross-section. There is little need to explicitly state the equivalent proportionality for the case of non-relativistic inverse bremsstrahlung, which reproduces the principal components of Eq. (11) in a similar manner. For normal bremsstrahlung from ultrarelativistic electrons, the integration can be performed with equal efficacy using Eq. (15), yielding

$$\left.\frac{dn_\gamma(\omega)}{dt}\right|_{\rm brems} \propto \frac{\Lambda\,\epsilon_e}{(\beta_{{\rm T},e})^{1-\Gamma_e}}\,\omega^{-\Gamma_e} \quad , \quad 1\lesssim\omega\,, \tag{A3}$$

thereby reproducing the form of Eq. (16), minus the complexity of integrations over the combinations of logarithmic and power-law factors.

REFERENCES

Allen, G. E. et al. 1997, ApJ 487, L97.
Baier, V. N., Fadin, V. S. & Khoze, V. A. 1967, Sov. Phys. JETP 24, 760.
Baring, M. G., Ellison, D. C. & Jones, F. C. 1993, ApJ 409, 327.
Baring, M. G., Ogilvie, K. W., Ellison, D. C., & Forsyth, R. J. 1997, ApJ 476, 889.
Baring, M. G., Ellison, D. C., Reynolds, S. P., Grenier, I. A., & Goret, P. 1999, ApJ 513, 311.
Bell, A. R. 1978, MNRAS 182, 147.
Boldt, E. 1987, Phys. Rep. 146, 215.
Boldt, E. & Serlemitsos, P. 1969, ApJ 157, 557.
Bethe, H. A. & Heitler, W. 1934, Proc. Roy. Soc. A146, 83.
Bloemen, H., et al. 1994, A&A 281, L5.
Bloemen, H., et al. 1999, to appear in Proc. 3rd Integral Workshop.
Blumenthal, G. R. & Gould, R. J. 1970, Rev. Mod. Phys. 42, 237.
Brown, R. L. 1970, ApJ 159, L187.
Cargill, P. J. & Papadopoulos, K. 1988, ApJ 329, L29.
Dogiel, V. A., et al. 1998, PASJ 50, 567.
Drury, L. O'C. 1983, Rep. Prog. Phys. 46, 973.
Eichler, D. 1984, ApJ 277, 429.
Ellison, D. C., Baring, M. G. & Jones, F. C. 1996, ApJ 473, 1029.
Ellison, D. C., Drury, L. O'C., & Meyer, J.-P. 1997, ApJ 487, 197.
Ellison, D. C., & Eichler, D. 1984, ApJ 286, 691.
Ellison, D. C., Goret, P., & Baring, M. G. 1999, in preparation.
Ellison, D. C., Möbius, E., & Paschmann, G. 1990, ApJ 352, 376.
Elwert, G. 1939, Ann. Physik 34, 178.
Fabian, A. C. & Barcons, X. 1992, Ann. Rev. Astr. Astrophys. 30, 429.
Fedyushin, B. K. 1952, Zhur. Eksp. Teor. Fiz. 22, 140.
Feldman, W. C. 1985, in Collisionless Shocks in the Heliosphere: Reviews of Current Research, Geophys. Monogr. Ser., 35, eds. B. T. Tsurutani and R. G. Stone (AGU, Washington, DC), p. 195.
Garibyan, G. M. 1952, Zhur. Eksp. Teor. Fiz. 24, 617.
Giacalone, J., Burgess, D. and Schwartz, S. J. 1992, in Proc. 26th ESLAB Symposium, Study of the Solar-Terrestrial System (ESA, Noordwijk) p. 65
Gould, R. J. 1970, Am. J. Phys. 38, 189.
Gradshteyn, I. S. and Ryzhik, I. M. 1980, Table of Integrals, Series and Products, (Academic Press, New York)
Green, D. A. 1998, A Catalogue of Galactic Supernova Remnants, (September 1998 edition) *http://www.mrao.cam.ac.uk/surveys/snrs/*
Haug, E. 1972, Astrophys. Lett. 11, 225.
Haug, E. 1975, Z. Naturforsch. 30a, 1099.
Hayakawa, S. 1969, Prog. Theor. Phys. 41, 1594.

Hayakawa, S. & Matsuoka, M. 1964, Prog. Theor. Phys. Suppl. 30, 204.
Helfand, D. J., Velusamy, T., Becker, R. H. & Lockman, F. J. 1989, ApJ 341, 151.
Hoang, S., Lacombe, C., Mangeney, A., Pantellini, F., Balogh, A., Bame, S. J., Forsyth, R. J. and Phillips, J. L. 1995, Adv. Space Sci. 15 (8/9), 371.
Hoshino, M., Arons, J., Gallant, Y. A., & Langdon, A. B. 1992, ApJ 390, 454.
Jauch, M. M. & Rohrlich, F. 1980, The Theory of Photons and Electrons, (2nd edn. Springer, Berlin)
Jones, F. C. 1971, ApJ 169, 503.
Jones, F. C. 1999, to appear in proc. of the Erice workshop on Cosmic Rays, eds. M. Shapiro et al., held in Erice, July 1998.
Jones, F. C. & Ellison, D. C. 1987, J. Geophys. Res. 92, 11,205.
Jones, F. C. & Ellison, D. C. 1991, Space Sci. Rev. 58, 259.
Jones, F. C., Jokipii, J. R. & Baring, M. G. 1998, ApJ 509, 238.
Keohane, J. W., Petre, R., Gotthelf, E. V., Ozaki, M., & Koyama, K. 1997, ApJ 484, 350.
Kim, K.-T., Kronberg, P. P. & Landecker, T. L. 1988, AJ 96, 704.
Koyama, K. et al. 1995, Nature 378, 255.
Marshall, F. E., et al. 1980, ApJ 235, 4.
Mason, G. M., Gloeckler, G., and Hovestadt, D. 1983, ApJ 267, 844.
Maxon, M. S. & Corman, E. G. 1967, Phys. Rev. 163, 156.
Meyer, J.-P., Drury, L. O'C., & Ellison, D. C. 1997, ApJ 487, 182.
Müller, D., & Tang, K.-K. 1987, ApJ 312, 183.
Müller, D., et al. 1995, Proc. 24th ICRC (Rome), 3, 13.
Pohl, M. 1998, A&A 339, 587.
Phillips, J. L., Bame, S. J., Gary, S. P., Gosling, J. T., Scime, E. E. & Forsyth, R. J. 1995, Space Sci. Rev. 72, 109.
Skibo, J. G., Ramaty, R. & Purcell, W. R. 1996, A&AS 120, 403.
Sommerfeld, A. 1931, Ann. Physik 11, 257.
Tanaka, Y., Miyaji, T.& Hasinger, G. 1999, Astron. Nachr., in press.
Tatischeff, V., Ramaty, R. & Kozlovsky, B. 1998, ApJ 504, 874.
Tatischeff, V., Ramaty, R. & Valinia, A. 1999, to appear in "LiBeB, Cosmic Rays and Gamma-Ray Line Astronomy", ASP Conference Series, eds. Ramaty, R., et al. [astro-ph/9903326]
Valinia, A., Kinzer, R. L. & Marshall, F. E. 1999, ApJ submitted.
Valinia, A. & Marshall, F. E. 1998, ApJ 505, 134.
Webber, W. R. 1997, Space Sci. Rev. 81, 107.
Weizsäcker, C. F. V. 1934, Zeit. für Physik 88, 612.
Williams, E. J. 1935, Kongelige Danske Vid. Selsk. Mat. Fys. Medd. 13, No. 4.
Wright, E. L., et al. 1994, ApJ 420, 450.
Zimmermann, H. U., Trümper, J. E., & Yorke, H. 1996, Röntgenstrahlung from the Universe, MPE Report 263 (Max-Planck-Institut für Extraterrestrische Physik, Garching).